Influence of a Receive-array Coil on Specific Absorption Rate at 3T: Simulations and Experiments with Basic Geometries

S. Oh[1], Y. Ryu[1], Z. Wang[2], F. Robb[2], and C. M. Collins[1]
[1]PSU College of Medicine, Hershey, PA, United States, [2]GE Healthcare, Aurora, OH, United States

Introduction: Receive-only (Rx) phased-array coils are used routinely in clinical situations for a number of purposes including achieving higher SNR [1] and shorter imaging times [2], but how their presence affects the RF field distribution during transmission is not routinely considered. At a minimum, the receive array introduces highly conductive surfaces with their associated boundary conditions for the electromagnetic fields from the transmit coil. Recent calculations considering realistic representations of actual arrays and considering their detuning circuits in detail have indicated that maximum local SAR can be up to 10% higher with the receive array present [3]. Given that most clinical studies include a receive array, better understanding of this relationship is required. Moreover, any defective detuning-circuit of a Rx-array could, in principle, result in greater SAR. In this work, numerical simulations and MR experiments were performed for a simple geometry (facilitating optimal match between geometries in simulation and experiment) to examine how the Rx-array coil can affect SAR in MRI.

Method: Numerical models of a transmit-only (Tx) head-sized birdcage coil containing a box-shaped phantom and either a) no Rx-array, b) a 2-element array with a gap in each coil to simulate perfect detuning, and c) a 2-element array with no gaps to simulate failed detuning were created using XFDTD software (Remcom, inc.). The grid had 2 mm resolution and the simulation was performed at 128 MHz. Details of the geometry are shown in Figure 1. The conductivity, relative permittivity, and weight of the phantom were 1.886 S/m and 77.52, and 843g, respectively. The phantom was placed in the 12-rung birdcage coil (diameter and length of shield/element were 320/280 and 380/296 mm, respectively). In previous work, simulations of this high-pass birdcage coil and the conductive agar-gel phantom (with no Rx-array) matched MR-based experimental measures of the SAR distribution well [4]. To simulate the Rx-array, two rectangular cooper loops were added at the top and bottom of the conductive agar-gel phantom with 2 mm space between the phantom surface and the copper-loop (Fig. 1). The two copper loops were connected by 2 mm-thick copper wire to simulate a common ground. To simulate ideal detuning, an air gap (2 mm) was modeled in each loop opposite the common ground. In a final simulation, the air gap was removed from the loops (creating a short circuit) to simulate a defective detuning condition. Results were scaled to have the same total dissipated power (in phantom) in all three cases. MR experiments were also performed on a 3 T whole-body MR system (Bruker, MA, USA). The experiments used practically identical geometry and phantom setting as in the numerical simulation. Maps of temperature increase were acquired on the center axial plane using the proton resonance frequency shift (PRF) method. Temperature maps were converted to SAR maps using a method described previously [4]. The matrix size, field of view, TR, TE, and slice thickness were 128×128, 170×170 mm^2, 100 ms, 10 ms, and 10 mm, respectively.

Results: Numerical calculations of SAR on the top coronal surface and mid-axial plane of the phantom in all three cases are shown in Figure 2. The experimentally acquired SAR maps of mid-axial planes are also shown in the bottom of Figure 2. Numerically calculated and experimentally acquired SAR maps match fairly well, with the round region of low SAR in the case with no Rx array becoming oblong in the vertical direction when the array is added and in the horizontal direction when the gap is closed for both methods. Results for the case with no Rx-array present show good agreement with the expected increase in SAR with the squared distance from the center, especially visible on the mid-axial plane. In simulation, the volume-averaged SAR (as reference SAR) was 0.2922 W/kg without the Rx-array. Addition of the Rx-array with ideal detuning caused obvious changes in the SAR distribution, most notable at the surface of the phantom. A region of very high SAR is seen near the gap placed for detuning. This is likely due to conservative electric fields resulting from a significant difference in charge density in the ends of the conductor separated by a gap. In this case, the volume-averaged SAR was 0.3022 W/kg, only 3% higher than with no Rx-array, but the peak SAR was 83% greater than the peak SAR with no Rx-array present. The defective detuning case shows significantly higher SAR than with no Rx-array, especially at the surfaces. In this case, the high SAR region near the (now closed) gap is not observed, and the peak SAR is only about 25% above that for the case with no Rx-array. However, significantly-increased SAR is observed over the majority of the surface of the phantom. The volume-averaged SAR of this case is 0.4119 W/kg, 41 % above that with no Rx-array present.

Discussion: This work presents some simple representations of a Rx-array against a phantom in a Tx coil for the purpose of developing some basic understandings of how the Rx-array can affect SAR and to allow for experimental validation of simulation methods. In practice, receive arrays are placed somewhat further from the subject than 2mm, and more sophisticated circuits are involved, but this simple case both demonstrates some basic phenomena and provides a scenario that should make a good case for experimental validation with previously-demonstrated methods in our future work.

Acknowledgement: This work was supported in part by the NIH through R01 EB000454.

References: [1] Roemer *et al*. Magn Reson in Med 1990;16:192-225
[2] Hoge *et al*. Concepts Magn Reson Part A 2005;27A:17-37
[3] Wang *et al.* 17th ISMRM 2009, Honolulu, USA, p. 3102
[4] Oh *et al*. 16th ISMRM 2008, Toronto, Canada, p. 79

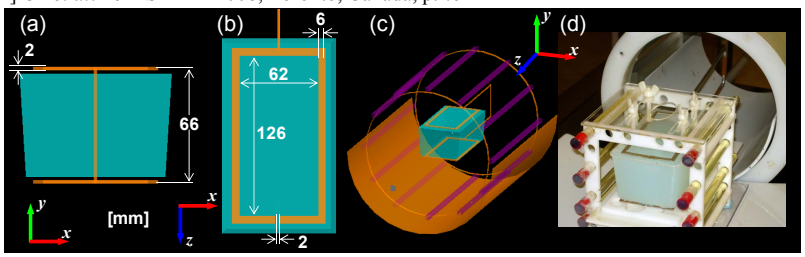

Figure 1. Geometry of phantom and Rx-array as viewed from (a) end, (b) above, and (d) 3D view of phantom and Rx-array in Tx birdcage coil with half of shield removed for improved visibility in XFDTD simulations. (d) View of experimental setup. Phantom and Rx-array were pulled out from birdcage coil for visibility. Reference phantoms (oil) are located at each side of agar phantom for spatially varying phase correction.

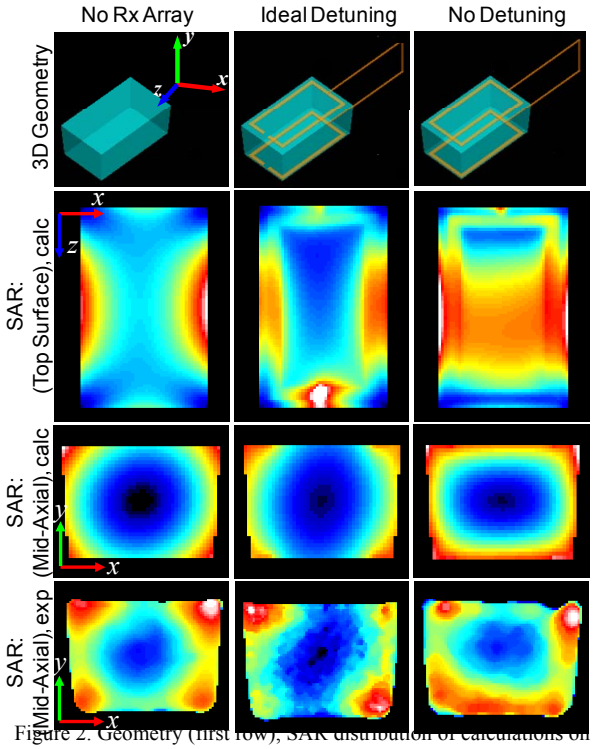

Figure 2. Geometry (first row), SAR distribution of calculations on top surface (second row), mid-axial plane (third row), and of experiments on mid-axial plane (forth row) for phantom in Tx coil without array (left column), phantom in Tx coil with perfectly-detuned array (middle column) and phantom in Tx coil with array having defective detuning (right column).